Data-Driven Characterization of EDFA In Constant Current Operation

Junho Cho[a], Jean-Christophe Antona[b], Alberto Bononi[c], and Paolo Serena[c]

[a] *Nokia Bell Labs, Holmdel, NJ 07733, USA (email: junho.cho@nokia-bell-labs.com)*
[b] *Alcatel Submarine Networks, Nojay, France (email: jean-christophe.antona@asn.com)*
[c] *Department of Engineering and Architecture, University of Parma, Parma, Italy (email: alberto.bononi@unipr.it, paolo.serena@unipr.it)*

(Invited)

***Abstract*—We study the electrical and optical characteristics of an EDFA designed for a latest submarine cable using a large set of measurement data. By clarifying dependence and independence of parameters, we demonstrate that an EDFA can be characterized numerically through few measurements.**

Keywords—EDFA, submarine cable, optical fiber communication

I. Introduction

Submarine optical fiber cables have been traditionally designed to maximize *fiber capacity* (i.e., the capacity of the individual fibers contained inside) rather than *cable capacity* (i.e., the aggregate capacity of all constituent fibers). Provisioning the maximum fiber capacity begins with a link design, including determination of span losses and launch power. Erbium-doped fiber amplifiers (EDFAs) are then designed to compensate for the determined span losses such that the electrical-to-optical power conversion efficiency (PCE) of the pump laser is maximized at the determined operating condition. High PCE is important for submarine systems, since only limited *electrical* power can be supplied from the shores to submarine EDFAs. However, maximizing cable capacity instead of fiber capacity demands a quite different design approach. In particular, substantially larger cable capacity can be obtained for a given total supply power by increasing the number of fibers in the cable [1], which involves reduction in optical launch power per fiber and individual fiber capacity. To maximize the cable capacity, a critical measure for each fiber is a different type of power efficiency m, defined as the fiber capacity per supply power [2]. Evaluation of m requires to measure the optical signal-to-noise ratio (SNR) at the cable termination, and hence to predict how optical power spectral density (PSD) will evolve as it passes through a series of submarine EDFAs for a given supply power, where gain flattening filters (GFFs) are not necessarily used. Therefore, an accurate simulator for EDFAs is essential to maximize the cable capacity, whose nominal operating condition can potentially be very different from the traditional conditions.

There are analytical EDFA models built with physical knowledge of absorption and emission behavior of erbium (see, e.g., [3]), which can be used as a simulator for submarine cable capacity maximization. However, its accuracy in predicting frequency-dependent gain is still an open question [1], [4]. There are machine learning approaches to EDFA modeling, where neural networks (NNs) are trained to enhance the prediction accuracy [4]. However, electrical power consumption has not been taken into account in prior works, which is needed for submarine cable capacity maximization. In this regard, we collected a set of large experimental data for a typical submarine EDFA at *fixed* pump currents, and built an accurate NN-based EDFA simulator to study the cable capacity maximization problem under a supply power constraint [5].

In this paper, using the large data set collected in [5], we characterize an EDFA designed for a latest submarine cable. A series of linear regressions is applied to characterize the EDFA, which gives useful insight into EDFA's amplification behavior. Clarification of various dependence and independence relations between parameters enables us to reduce the training data size for an NN-based EDFA simulator. The EDFA characterization also allows to directly build a numerical EDFA simulator, as presented in this paper.

II. Experimental Setup for Data Acquisition

The large data set in [5] was obtained in the following manner, using the same emulator of the wavelength-division multiplexing (WDM) transmitter (TX) as in [1, Fig. 1]. A high-power frequency-flat amplified spontaneous emission (ASE) is generated by using three cascaded EDFAs, and the PSD of the ASE is carved by using two cascaded wavelength switches (WSSs), such that high-power emulated-signal bands S_I at 50-GHz-wide frequency bins (blue circles in Fig. 1) and low-power noise bands N_I at 50-GHz-wide frequency bins (orange squares in Fig. 1) alternately appear 40 times to fill 4 THz in the C-band in a piecewise frequency-flat manner. A subsequent EDFA and a variable optical attenuator (VOA) rectifies the total optical power of the emulated WDM TX power profile to make a target value P_I. The emulated WDM TX power profile then passes through an EDFA under test operating at two different constant pump currents $I_{Pump} =$ 150 mA and 450 mA (resulting in constant *electrical* pump powers of 205 mW and 675 mW). At the output of the EDFA under test, the signal powers $S_O(k)$ and noise powers $N_O(k)$ are measured by using an optical spectrum analyzer (OSA), where $k = 1, \dots, 80$ denotes the frequency band index and the subscripts $\{\cdot\}_I$ and $\{\cdot\}_O$ indicate whether the power is measured at the input or output of the EDFA. We send 21,200 different power profiles $[S_I(k), N_I(k)]$ through the EDFA, whose piecewise flat PSDs randomly fluctuate with a maximum signal power excursion ΔS_I of 28 dB and a maximum noise power excursion ΔN_I of 12 dB (cf. Fig. 1). The mean SNR of the TX power profiles, defined as the ratio of the total signal power to the total noise power, varies over

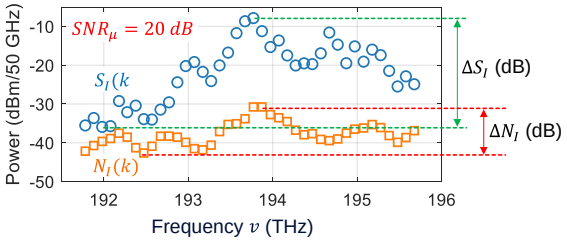

Fig. 1. An example of 21,200 random WDM TX power profiles.

978-1-7281-5445-9/20/$31.00 ©2020 IEEE

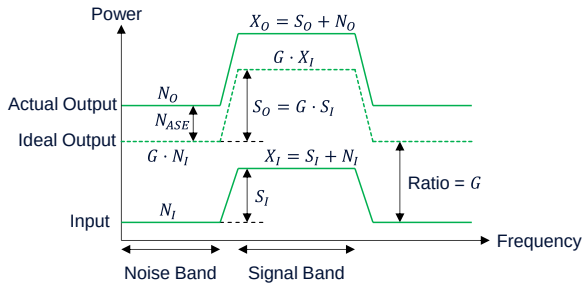

Fig. 2. A schematic showing the definitions of $S_{I/O}$, $N_{I/O}$, N_{ASE}, and G.

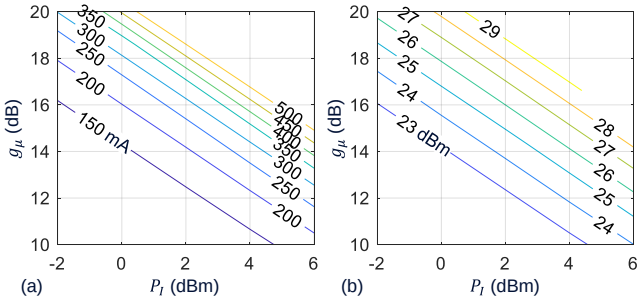

Fig. 3. (a) Pump current and (b) pump power required to obtain g_μ.

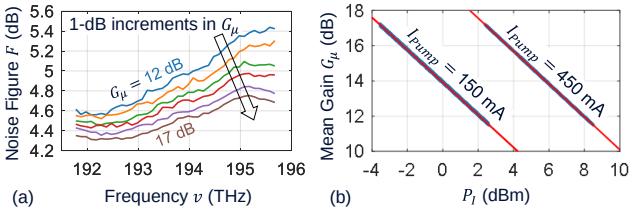

Fig. 4. (a) Noise figure, and (b) mean gain G_μ of the EDFA.

a range of 52 dB. The large power excursions ΔS_I and ΔN_I are to investigate how the EDFA behaves differently as the input PSD changes, and the large SNR variation is to ensure that the characterization is valid no matter where the EDFA is placed on a transoceanic distance.

III. Characterization of EDFA

A. EDFA Gain and Noise Figure

With reference to the schematic diagram in Fig. 2, we note that we can measure only the noise powers $N_{I/O}(k)$ in noise bands (where $S_{I/O}(k) = 0$) and only the mixture of signal and noise powers $X_{I/O}(k) = S_{I/O}(k) + N_{I/O}(k)$ in signal bands. In signal bands, $N_{I/O}(k)$ and $S_{I/O}(k)$ mask each other, and thus we determine $N_{I/O}(k)$ by interpolating $N_{I/O}(k-1)$ and $N_{I/O}(k+1)$ measured in the adjacent noise bands (cf. Fig. 2) and then determine $S_{I/O}(k)$ through $S_{I/O}(k) = X_{I/O}(k) - N_{I/O}(k)$. The gain $g(k)$ of an EDFA at frequency band k has often been defined as the ratio of the output power to the input power in the band, i.e., $g(k) = X_O(k)/X_I(k)$. Similarly, the mean gain g_μ of an EDFA is obtained from the total input power $P_I = \sum_k X_I(k)$ and the total output power $P_O = \sum_k X_O(k)$ as $g_\mu = P_O/P_I$. This definition is useful since by making g_μ the same as the span loss, P_O can be made the same as the launch power at every span. Figure 3 depicts the mean gain g_μ of our EDFA under test measured at various conditions, showing that as P_I increases, the EDFA consumes more pump power for the same g_μ.

In this paper, we use a slightly different EDFA gain defined as the ratio of the output *signal* power to the input *signal* power, i.e.,

$$G(k) = S_O(k)/S_I(k), \tag{1}$$

quantifying the *net gain* from the perspective of signal. From this definition and the amplifier physics, we have the following relations (cf. Fig. 2):

$$S_O(k) = G(k)S_I(k), \tag{2}$$

$$N_{ASE}(k) = G(k)F(k)h\nu B_0, \tag{3}$$

$$\begin{aligned} N_O(k) &= G(k)N_I(k) + N_{ASE}(k) \\ &= G(k)[N_I(k) + F(k)h\nu(k)B_0], \end{aligned} \tag{4}$$

$$\begin{aligned} X_O(k) &= S_O(k) + N_o(k) \\ &= G(k)[X_I(k) + F(k)h\nu(k)B_0], \end{aligned} \tag{5}$$

where $N_{ASE}(k)$ is the ASE noise power in the k-th bin, $F(k)$ denotes the noise figure (NF) of the k-th bin as defined in ITU [6], h is the Planck constant, $\nu(k)$ is the center frequency of the k-th bin, and $B_0 = 50$ GHz is the noise bandwidth. The gain $g(k)$ is associated with $G(k)$ as $g(k) = G(k) + N_{ASE}(k)/X_I(k)$, and hence can be approximated as $g(k) \approx G(k)$ when $N_{ASE}(k)/X_I(k) \approx 0$. This approximation is valid for traditional submarine systems that use GFFs to realize a flat PSD over the whole distance. However, it does not necessarily hold in more general systems that do not realize a flat PSD and hence $X_I(k)$ in some bands can be very small, especially with a small P_I due to massively parallel fibers; e.g., $N_{ASE}(k)/X_I(k)$ as high as 0.25 is observed in our measurement data.

From Eq. (5), the NF can be determined from measurements as $F(k) = [X_O(k)/G(k) - X_I(k)]/(h\nu(k)B_0)$. We assume that $F(k)$ is a function only of k at a fixed *mean gain* $G_\mu = \sum_k S_O(k) \,/\, \sum_K S_I(k)$, independent of P_I or the distribution of the input PSD. This assumption is justified by the fact that $F(k)$ is a function only of $G(k)$ and that $G(k)$ is a function only of k at a fixed G_μ, the latter of which will be demonstrated below. We determine $F(k)$ by using only a small selected data set with the highest input SNRs (thus with the highest $S_I(k)$ for a fixed P_I) to ensure high accuracy in estimating $G(k)$ from measurements. Figure 4(a) shows such determined $F(k)$ of our EDFA.

B. Charaterizing Gain by Successive Linear Regression

We then characterize $G(k)$ for all the input power profiles, by successively applying linear regression. Throughout the paper, linear regression is based on the *least-squares* method. Following the convention, we first factorize $G(k)$ as $G(k) = G_\mu \cdot G_T(k) \cdot G_R(k)$, where G_μ is the mean gain , $G_T(k)$ is the *gain tilt* that characterizes the linear dependence of log-scale $G(k)$ on frequency $\nu(k)$, and $G_R(k)$ is the residual gain factor called the *gain ripple*. Denoting G expressed in decibels by G^{dB}, the gain factorization can be written as $G^{dB}(k) = G_\mu^{dB} + G_T^{dB}(k) + G_R^{dB}(k)$.

Figure 4(b) shows G_μ^{dB} of the EDFA obtained from 21,200 measurement data for each I_{Pump}, where each blue dot represents one measurement data and the red lines are the linear fits. Figure 4(b) clearly shows that for a fixed I_{Pump}, G_μ^{dB} is merely a linear function of P_I^{dBm}, and is not affected by the large signal and noise power excursions.

By definition, the gain tilt characterizes the linear relation between $G^{dB}(k)$ and ν, and thus can be expressed using slope a and y-intercept b as $G_T^{dB}(k) = a[\nu(k) - \nu_0] + b$, where we choose $\nu_0 = 194$ THz as a reference frequency in this work. Figure 5 shows a and b obtained from the measurement data. It can be seen that for a fixed G_μ^{dB}, the gain tilt G_T^{dB} is almost independent of the random excursions of $S_I(k)$ and $N_I(k)$;

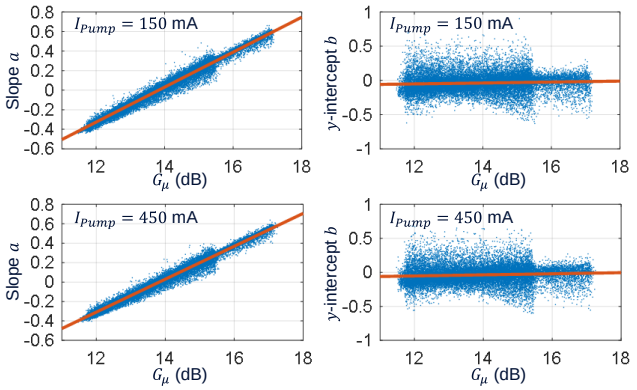

Fig. 5. Slope a and y-intercept b of G_T^{dB} at I_{Pump} = 150 mA (top) and 450 mA (bottom).

instead, a and b can be approximated as a linear function *only* of G_μ^{dB}, independently of the two considered I_{Pump}. The larger spread of a and b at $G_\mu^{dB} \leq 15.5$ is simply because there are more data points. The linear regression errors in Fig. 5 seem to be large, but numerical characterization of the EDFA with this linear regression produces an excellent performance in predicting output PSDs, as will be shown below. We attribute the large deviations around their linear fits to the fact that the WSSs of the TX emulator cannot produce ideal piecewise flat PSDs and the EDFA distorts the piecewise flatness of the PSD due to a non-flat gain, both of which can incur inaccuracy in measurement.

Figure 6 shows the gain, and its constituent tilt and ripple for various G_μ, obtained with linear regressions on the 21,200 measurement data for I_{Pump} = 150 mA. The curves for I_{Pump} = 450 mA are nearly identical to those of Fig. 6.

C. Prediction of Output PSD

Characterization of an EDFA with a small number of measurements is immediate from the above findings. First, we determine the linear function l_μ such that $G_\mu^{dB} = l_\mu(P_I^{dBm})$ (cf. red lines in Fig. 4(b)), by varying P_I^{dBm} for each I_{Pump}. At a chosen I_{Pump}, which can represent any I_{Pump} in our EDFA characterization, we pick a range of G_μ^{dB} of interest, e.g., $G_\mu^{dB} \in \{12, \ldots, 17\}$, and determine the linear functions l_a and l_b such that $a = l_a(G_\mu^{dB})$ and $b = l_b(G_\mu^{dB})$ (cf. red lines in Fig. 5) and the residual gain ripples $G_R^{dB}(k)$ (cf. Fig. 6(c)). In our test conditions, this can be done by launching $X_I(k)$ that have just 7 different P_I^{dBm} with flat $X_I(k)$ in signal bands.

To predict the output PSD for an arbitrary input PSD at a given I_{Pump}, we calculate P_I^{dBm} and obtain G_μ^{dB} for the given I_{Pump} by interpolating $l_\mu(P_I^{dBm})$ of various I_{Pump} (cf. Fig. 4). Having G_μ^{dB}, we calculate $a = l_a(G_\mu^{dB})$ and $b = l_b(G_\mu^{dB})$ and obtain $G_T^{dB}(k) = a[v(k) - v_0] + b$. The gain ripple $G_R^{dB}(k)$ for the given G_μ^{dBm} can then be obtained by linearly interpolating the predetermined $G_R^{dB}(k)$ curves with respect to G_μ^{dBm} at each k. Eventually, we obtain $G^{dB}(k) = G_\mu^{dB} + G_T^{dB}(k) + G_R^{dB}(k)$, and produce the estimate $\tilde{X}_O(k)$ using $G(k)$, $F(k)$, and $X_I(k)$ based on Eq. (5). Figure 7 depicts the probability density function (PDF) of prediction error $E^{dB}(k) = \tilde{X}_O^{dBm}(k) - X_O^{dBm}(k)$ and the complementary cumulative density function (CCDF) of absolute errors $|E^{dB}(k)|$ at I_{Pump} = 150 mA, showing that $|E^{dB}(k)| \leq 0.47$ dB with 99% probability. The root-mean-square (RMS) error is 0.14 dB. The prediction errors for I_{Pump} = 450 mA show very similar probabilities as in Fig. 7.

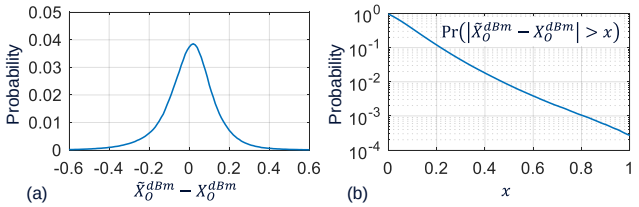

Fig. 7. (a) PDF of the prediction error, and (b) CCDF of the absolute prediction error, both at I_{Pump} = 150 mA.

IV. Conclusion

By using extensive measurement data, we showed that the spectral gain shape of an EDFA is determined solely by the mean gain G_μ, independently of the shape of the input PSD or the total optical input power. In the lack of this physical knowledge, training NNs to learn the EDFA's behavior requires a complicated topology and a huge set of measurement data. However, the knowledge of the dependence and independence relations enables us to greatly simplify the topology of the NNs and substantially alleviate the daunting measurement task. It also enables a classical regression approach to characterize the EDFA with high accuracy, as we verified by predicting output PSDs for arbitrary input PSDs with only 0.14 dB of the RMS error.

References

[1] J. Cho et al., "Supply-power-constrained cable capacity maximization using multi-layer neural networks," *J. Lightw. Technol.*, vol. 38, no. 14, pp. 3652-3662, Jul. 2020.

[2] A. Turukhin et al., "Power-efficient transmission using optimized C+L EDFAs with 6.46 THz bandwidth and optimal spectral efficiency," in *Proc. ECOC*, Rome, Italy, Sep. 2018, Paper Mo.4.G.4.

[3] A. A. M. Saleh et al., "Modeling of gain in erbium-doped fiber amplifiers," *IEEE Photon. Technol. Lett.*, vol. 2, no. 10, pp. 714-717, Oct. 1990.

[4] S. Zhu et al., "Machine learning based prediction of erbium-doped fiber WDM line amplifier gain spectra," in *Proc. ECOC*, Rome, Italy, Sep. 2018, Paper Mo.3.E.6.

[5] J. Cho et al., "Optimizing gain shaping filters with neural networks for maximum cable capacity under electrical power constraints," submitted for publication.

[6] D. M. Baney et al., "Theory and measurement techniques for the noise figure of optical amplifiers," *Opt. Fiber Technol.*, vol. 6, no. 2, pp. 122-154, Apr. 2000.

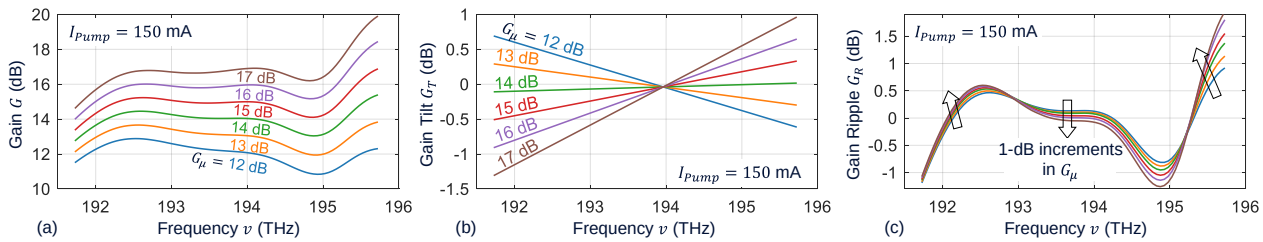

Fig. 6. (a) Gain $G(k)$, (b) gain tilt $G_T(k)$, and (c) gain ripple $G_R(k)$ of the EDFA operating at I_{Pump} = 150 mA.